Osteoarthritis and Cartilage xxx (2015) 1–9

Osteoarthritis and Cartilage

OARSI OSTEOARTHRITIS RESEARCH SOCIETY INTERNATIONAL

# Iron overload in a murine model of hereditary hemochromatosis is associated with accelerated progression of osteoarthritis under mechanical stress

A. Camacho † ‡ ‖ *, M. Simão ‖ ¶, H.-K. Ea # ††, M. Cohen-Solal # ††, P. Richette # ††, J. Branco ‡‡ §§, M.L. Cancela § ‖

† *Department of Orthopedics, Centro Hospitalar Lisboa Central, Lisboa, Portugal*
‡ *PhD Program in Medicine, NOVA Medical School, University Nova de Lisboa, Lisbon, Portugal*
§ *Department of Biomedical Sciences and Medicine (DCBM), University of Algarve, Faro, Portugal*
‖ *Centre of Marine Sciences (CCMAR), University of Algarve, Faro, Portugal*
¶ *PhD Program in Biomedical Sciences, University of Algarve, Faro, Portugal*
# *Inserm 1132, Hôpital Lariboisière, Paris, France*
†† *Université Paris Diderot, UFR médicale, Assistance Publique-Hôpitaux de Paris, Hôpital Lariboisière, Fédération de Rhumatologie, Paris, France*
‡‡ *Department of Rheumatology, Hospital Egas Moniz, Centro Hospitalar Lisboa Ocidental EPE, Lisbon, Portugal*
§§ *CEDOC – Chronic Diseases Research Center, NOVA Medical School, University Nova de Lisboa, Lisbon, Portugal*

ARTICLE INFO

*Article history:*
Received 8 June 2015
Accepted 11 September 2015

*Keywords:*
Iron overload
Mouse model
Hereditary hemochromatosis
Osteoarthritis
Mechanical stress

SUMMARY

*Objective:* Hereditary hemochromatosis (HH) is a disease caused by mutations in the *Hfe* gene characterised by systemic iron overload and associated with an increased prevalence of osteoarthritis (OA) but the role of iron overload in the development of OA is still undefined. To further understand the molecular mechanisms involved we have used a murine model of HH and studied the progression of experimental OA under mechanical stress.

*Design:* OA was surgically induced in the knee joints of 10-week-old C57BL6 (wild-type) mice and *Hfe*-KO mice. OA progression was assessed using histology, micro CT, gene expression and immunohistochemistry at 8 weeks after surgery.

*Results:* *Hfe*-KO mice showed a systemic iron overload and an increased iron accumulation in the knee synovial membrane following surgery. The histological OA score was significantly higher in the *Hfe*-KO mice at 8 weeks after surgery. Micro CT study of the proximal tibia revealed increased subchondral bone volume and increased trabecular thickness. Gene expression and immunohistochemical analysis showed a significant increase in the expression of matrix metallopeptidase 3 (MMP-3) in the joints of *Hfe*-KO mice compared with control mice at 8 weeks after surgery.

*Conclusions:* HH was associated with an accelerated development of OA in mice. Our findings suggest that synovial iron overload has a definite role in the progression of HH-related OA.



## Introduction

Osteoarthritis (OA) is a disease of the joints characterized by progressive articular cartilage destruction and subchondral bone changes. Several factors influence OA development, including genetic background, past joint injuries, mechanical overload and ageing[1,2]. The pathologic process that leads to cartilage destruction involves a disruption of the normal resting state of chondrocytes, leading to an increased production of both matrix proteins and matrix degrading enzymes such as matrix metallopeptidase (MMP) and a disintegrin and metallopeptidase with thrombospondin motifs (ADAMTS)[3].

Hereditary hemochromatosis (HH), a chronic disease caused by mutations in the *Hfe* gene[4] and characterized by systemic iron overload that causes damage in the liver, heart and endocrine organs[5], is associated with an increased incidence of OA[6] and joint replacement surgery[7–9]. Although liver and heart complications are the main causes of mortality in patients with HH, arthropathy has the greatest impact on the quality of life and rarely benefits

* Address correspondence and reprint requests to: A. Camacho, Department of Orthopedics, Centro Hospitalar Lisboa Central, Rua da Beneficência, n.º 8, 1069-166 Lisboa, Portugal. Tel: 351-217-924-200.
*E-mail address:* antonio.camacho@chlc.min-saude.pt (A. Camacho).

http://dx.doi.org/10.1016/j.joca.2015.09.007
1063-4584/

from therapeutic phlebotomies[10]. Studies of human joint tissue have shown hemosiderin accumulation in the cartilage and synovial tissue and histological features reminiscent of OA and of rheumatoid arthritis (RA)[11,12] and increased ferritin levels in the synovial fluid[13] of affected joints, but it is unclear how the iron overload damages the joints and which HH patients will develop musculoskeletal complications[14].

Previous reports have shown that murine models of HH can be useful in studying the pathogenesis of HH-related liver disease[15], HH-related diabetes[16] and HH-related changes in bone metabolism[17], but there are no studies using a murine model of HH to investigate the effect of iron overload in articular cartilage.

In order to investigate the role of iron overload in the development of OA we induced OA[18] in a mouse model of HH[19] and studied the subsequent morphological, histological and genetic changes occurring in the cartilage and subchondral bone of the knee joint.

## Materials and methods

Details of additional data, methods, primers and reagents are available in the Supplementary information material.

### *Animal model, experimental procedure, feeding and housing*

The *Hfe*-KO mice in a C57BL/6 background[19] (HFE-KO) were used as a model for human HH. C57Bl/6 mice from the University of Algarve Animal Facility in-house colony were used as wild-type controls. Distribution of animals between groups and tasks is further explained in Supplementary fig. 1. Animals were maintained in specific pathogen-free conditions and had access to water and food *ad-libitum* from weaning up to time of euthanasia. OA was induced in the right knee joint of 10-week-old Hfe-KO and wild-type mice by sectioning the medial collateral ligament and excising of the medial meniscus (MNX) using a microscope[18]. The left knee was sham-operated (SHAM). All the animals were euthanized 8 weeks after surgery and bilateral knee joints were collected, processed and used as described below. All the procedures were approved by the Portuguese National Authority for Animal Health (Ref. 0421/000/000/2013) and by the Animal Facility of University of Algarve.

### *Assessment of iron accumulation*

For the assessment of iron accumulation in the liver and blood, samples of six animals of each strain were used. At the time of euthanasia blood was collected by intra-cardiac puncture for determination of serum iron, serum ferritin and serum transferrin saturation; liver tissue was collected to determine the hepatic non-heme iron concentration[20].

### *Grading of osteoarthritic changes*

Bilateral knee joints from ten animals in each group were isolated, cleaned of adherent soft tissues in ice-cold PBS and fixed for 24 hrs in 4% paraformaldehyde in PBS pH 7.4, followed by decalcification with 0.5 M Ethylenedinitrilotetraacetic acid (EDTA) in PBS pH 7.4 for 3 weeks. After dehydration through graded alcohols and inclusion in paraffin, 5 μm sagittal sections were cut from the medial compartment of the joints and stained with Safranin-O/Fast Green/Meyer's Hematoxylin. Two separate observers, blinded to the strain and intervention, graded the cartilage lesions (grade 0–6) using the Osteoarthritis Research Society International (OARSI) scoring system for murine OA[21]. The medial tibial plateau and the medial femoral condyle were graded separately. The final score for each joint was the average of both observers score.

### *Morphological characterization of the knee joint by micro-CT*

Micro-CT was performed on bilateral knee joints of five animals in each group with a Skyscan 1172 X-ray computed microtomograph (Bruker, Belgium). For the image acquisition the following parameters were used: X-ray tube potential 70 kVp, X-ray tube current 100 μA, 0.5 mm Al filter, rotation step 0.4°, isotropic voxel size 5 $\mu m^3$, integration time 500 ms, frame averaging = 6. The proximal epiphysis of the tibia was selected as region of interest (ROI). To quantify the characteristics of the subchondral bone[22] the epiphysis was further divided in a cortical part (subchondral bone plate) and a trabecular part. The following 3D morphometric parameters were used to describe the bone of the trabecular compartment: Bone volume fraction (BV/TV, in %) is the ratio of the segmented bone volume to the total volume of the region of interest; Connective density (Conn.D, in $mm^{-3}$) is a measure of the average number of trabeculae per unit of volume; Trabecular thickness (Tb.Th, in μm) is the mean thickness of trabeculae. To describe the subchondral bone plate we measured the average thickness (Sb.Th, in μm).

### *Histological evaluation of undecalcified samples*

Following micro-CT the samples were included in methyl methacrylate (MMA) at 4°C. From these undecalcified samples, 5 μm sagittal sections were cut from the medial knee compartment on a heavy-duty microtome equipped with tungsten carbide knives. Sections were stained with Perl's and counterstained with Neutral Red in order to assess iron deposition. The regions of interest for this analysis were the knee joint and the proximal epiphysis of the tibia. The total area of hemosiderin deposits in the synovial membrane was measured as previously described[11].

### *Evaluation of gene expression*

The bilateral knee joints of ten mice from each strain were used for RNA isolation. Immediately after euthanasia both knee joints were immersed in RNALater at 4°C and cleaned of soft tissues, in order to isolate the tibial and femoral cartilage and subchondral bone of the medial knee compartment. RNA was extracted using TRI Reagent (Sigma–Aldrich), purified using the High Pure RNA Isolation Kit (Roche) and quantified with an Experion RNA analysis system (Bio-Rad). The reverse transcription reaction (RT) was carried out using 0.5 μg of total RNA per reaction with the M-MLV reverse transcriptase (Invitrogen) according to the manufacturer indications. Real-time PCR was carried out in a Bio-Rad CFX-96 machine, using the parameters specified by the manufacturer for the combination of machine and master mix. The *Rpl13a* gene was used as control of endogenous gene expression[23] and the WT.SHAM group as the reference condition.

### *Immunohistochemistry*

Bilateral knee joints of three mice of each strain were used for immunohistochemical localization. After dewaxing and rehydration, epitope retrieval was performed and the sections were incubated with polyclonal rabbit antibodies against mouse MMP-3, MMP-13 (Proteintech, England), ADAMTS-5 (Abcam ab41037) at a dilution of 1:40 and against type X collagen (Abcam ab58632) at a dilution of 1:20 for 24 h at 4°C. The sections were then treated with 0.3% hydrogen peroxide to block endogenous peroxidases, incubated with horseradish peroxidase-conjugated goat antibodies against rabbit IgG (Sigma–Aldrich) at a 1:100 dilution. After rinsing, the sections were incubated with a 0.05% 3,3′-diaminobenzidine solution to visualize the location of the target

Please cite this article in press as: Camacho A, et al., Iron overload in a murine model of hereditary hemochromatosis is associated with accelerated progression of osteoarthritis under mechanical stress, Osteoarthritis and Cartilage (2015), http://dx.doi.org/10.1016/j.joca.2015.09.007

protein-primary-secondary antibodies complex and counter-stained with Mayer's haematoxylin.

*Statistical analysis*

Unless stated otherwise, results are expressed as the mean and corresponding 95% Confidence Interval (95% CI). The Student's-*t* test was used to compare continuous variables between different strains. The Mann-Whitney *U* test was used when comparing ordinal variables or when the assumptions for a parametric test were not met. Pairwise comparisons using paired *t*-tests with Holm's *P*-value adjustment were used to compare continuous variables between different groups, in order to account for the correlation between joints of the same animal. The Wilcoxon paired test with Holm's *P*-value adjustment was used for ordinal variables. A two-tailed *P*-value $< 0.05$ was considered statistically significant. All analysis and plotting were conducted using the R v3.1.1 (R Foundation for Statistical Computing, Vienna, Austria) software.

## Results

All the animals initially operated were included in the final analysis; the experimental procedure had no adverse effects on the mice.

*Mice not expressing the Hfe allele have increased iron accumulation in the serum, liver and knee synovial membrane*

The Hfe-KO mice had a plasmatic iron overload ($n = 6$ per group, Fig. 1(A)) and up to five fold increase in hepatic iron content when compared to their controls [1121, 95% CI (927, 1316) μg iron/mg of wet liver weight vs 282, 95% CI (196, 367) μg iron/mg of wet liver weight; *P*-value = 0.002, respectively, $n = 6$ per group].

To evaluate the iron accumulation in the joints of Hfe-KO mice we used undecalcified, MMA-embedded sections of the knee, stained with Perl's. We observed hemosiderin deposits in the synovial membrane of the knee but not in the cartilage (Supplementary fig. 2). These occupied a greater area in the Hfe-KO mice, although there was no significant difference between the MNX and the SHAM operated sides ($n = 5$ per group, Fig. 1(B)). Unpublished data from our research team (Simão M) showed that in non-operated knees of Hfe-KO mice there is no accumulation of hemosiderin in the synovial membrane at 18 weeks of age (Supplementary fig. 3). These observations suggest that the hemosiderin deposits originate from the blood that enters the joint following the arthrotomy. The higher iron content of the Hfe-KO mice blood could explain the greater hemosiderin accumulation.

Using RNA extracted from the subchondral bone and articular cartilage we examined the *Hfe* and *Tfrc* mRNA expression. Real-time PCR analysis confirmed the decreased *Hfe* expression in the Hfe-KO

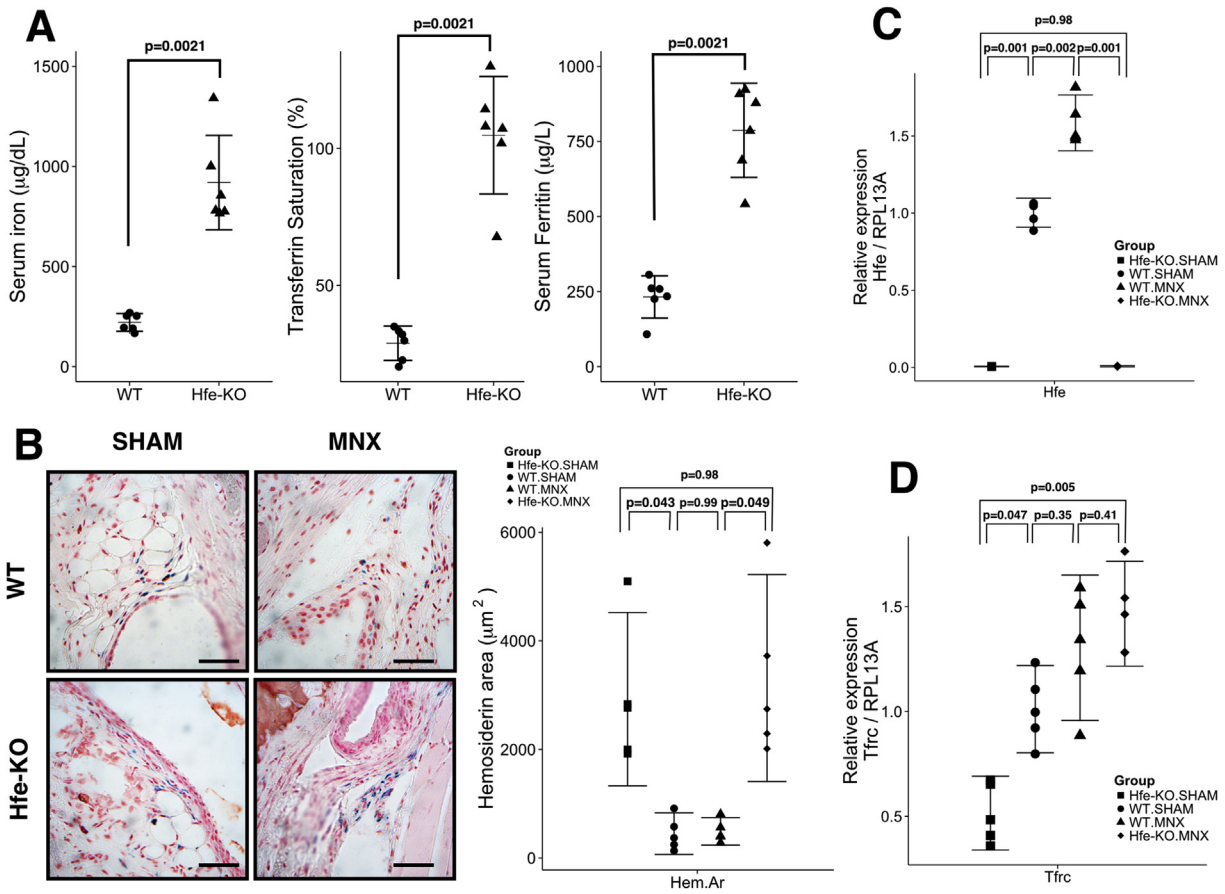


**Fig. 1.** Iron parameters in WT and Hfe-KO mice (A) Bar plots for the different serum iron parameters. (B) Perl's staining of MMA-embedded knee joint, high magnification view of the knee synovial membrane to observe the hemosiderin deposits (blue) and the quantification of their area showing a greater accumulation of iron in the synovial membrane of the Hfe-KO mice. Scale bar 50 μm. (C) Real time PCR, using mRNA isolated from the medial knee compartment of 18 weeks-old animals, to detect the expression of the *Hfe* gene in the Hfe-KO and control animals ($n = 5$ per group). The results confirm that the *Hfe* gene is not expressed in the bone and cartilage of the Hfe-KO mice. (D) Real time PCR, using mRNA isolated from the medial knee compartment of 18 weeks-old animals, to detect the expression of the *Tfrc* gene. The results show that in Hfe-KO there is an underexpression of the *Tfrc* gene and that the medial meniscectomy leads to an overexpression of this gene. Data are shown as the individual values (shapes) with the corresponding 95% CI (range).

Please cite this article in press as: Camacho A, et al., Iron overload in a murine model of hereditary hemochromatosis is associated with accelerated progression of osteoarthritis under mechanical stress, Osteoarthritis and Cartilage (2015), http://dx.doi.org/10.1016/j.joca.2015.09.007

mice ($n = 5$ per group, Fig. 1(C)). The *Tfrc* expression was decreased in the Hfe-KO SHAM-operated knees and was elevated in both strains on the MNX-operated knees. ($n = 5$ per group, Fig. 1(D)).

### *Hfe-KO mice have increased cartilage degeneration and subchondral bone volume following the surgical induction of OA*

The Hfe-KO mice were morphologically indistinguishable from their WT counterparts and had similar body weight at the time of euthanasia [24.5, 95% CI (23.4, 25.6) g vs 25.2, 95% CI (24.3, 26.1) g respectively; *P*-value = 0.33; $n = 28$ per strain].

To evaluate the effect of the iron overload in the development of OA we surgically induced OA in Hfe-KO mice and in WT controls, using a previously described technique[18]. At 8 weeks after the intervention the MNX-operated knees of the Hfe-KO mice showed a higher level of cartilage destruction [Fig. 2(A)], resulting in a higher summed tibial and femoral OARSI scores for the medial femoral condyle and medial tibial plateau ($n = 10$ per group, Fig. 2(B)). We assessed the articular calcified cartilage (ACC) and the hyaline articular cartilage (HAC) of the tibial plateau in the undecalcified, MMA-embedded knee sections. The MNX operated knees had a lower ACC thickness, lower HAC/ACC ratio and greater subchondral bone height ($n = 5$ per group, Supplementary fig. 4).

To better evaluate the subchondral bone architecture of the medial tibial plateau, we performed micro-CT scans of the knee joints [Fig. 3(A)]. The MNX-operated knees in both strains showed an increase in bone volume, in trabecular thickness and in subchondral plate thickness, but these increases were greater in the Hfe-KO mice ($n = 5$ per group, Fig. 3(B)).

Using RNA extracted from the subchondral bone and articular cartilage we examined *Bmp6* mRNA expression, a signalling molecule involved in iron homeostasis[24] and bone formation[25] and found it to be increased in the Hfe-KO MNX operated knees compared to their WT controls ($n = 5$ per group, Fig. 3(C)). These findings suggest that the Hfe-KO animals have an accelerated progression of the experimental OA, when compared to their WT controls.

### *The expression of a gene related to cartilage degradation is increased in knee joints of the Hfe-KO mice*

To have a better understanding of the accelerated progression of the articular damage in the Hfe-KO mice, we investigated the expression of genes known to be involved in the acute inflammatory response and in the development of OA, namely genes coding for components of the extracellular matrix, chondrocyte hypertrophic markers, factors that promote bone formation, cartilage-degrading enzymes and pro-inflammatory cytokines.

Although cytokines Il1b and Il6 showed no meaningful change in expression at 8-weeks post surgery (Supplementary fig. 5), the remaining genes were up regulated in all MNX-operated knees ($n = 5$ per group, Fig. 4). Only *Mmp3*, a cartilage-degrading enzyme, was up regulated in the Hfe-KO, MNX operated knees when compared with their WT.MNX controls, at 8 weeks after surgery ($n = 5$ per group, Fig. 4).

In addition, we evaluated the localization of some of the proteins encoded by these genes using immunohistochemical staining. Eight weeks after surgery both the Hfe-KO and the WT MNX

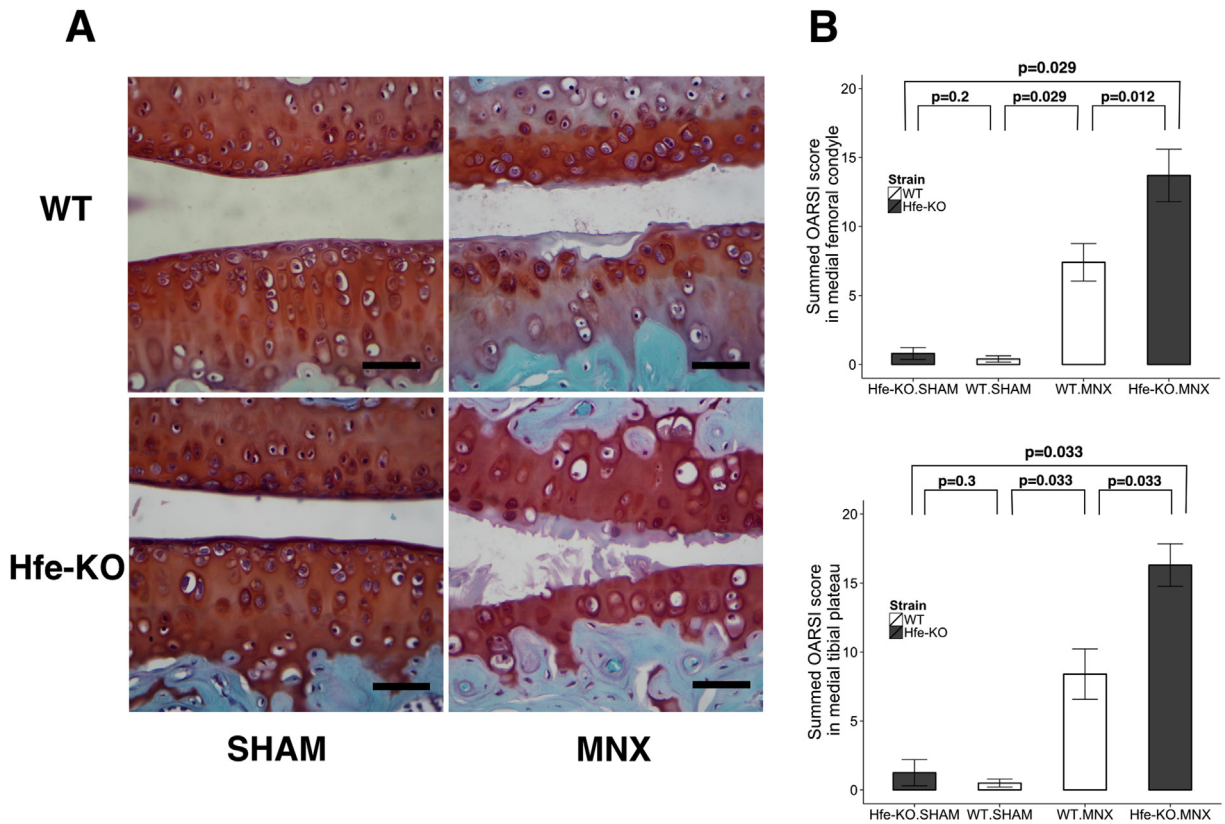


**Fig. 2.** Cartilage changes following meniscectomy in WT and Hfe-KO mice (A) Haematoxylin-Fast Green-Safranin-O staining of the medial femoral condyle and tibial plateau of control ($n = 10$ per group) and Hfe-KO mice ($n = 10$ per group) at 8 weeks after surgical induction of OA. Scale bar 50 μm. (B) The Osteoarthritis Research Society International (OARSI) scores for the medial femoral condyle and medial tibial plateau of control and Hfe-KO mice (SHAM and MNX operated knees) were obtained by summing the score of three sections from the lateral, middle and medial one-third of the medial knee compartment from each mouse. Data are shown as the mean (bar) and corresponding 95% CI (range).

Please cite this article in press as: Camacho A, et al., Iron overload in a murine model of hereditary hemochromatosis is associated with accelerated progression of osteoarthritis under mechanical stress, Osteoarthritis and Cartilage (2015), http://dx.doi.org/10.1016/j.joca.2015.09.007

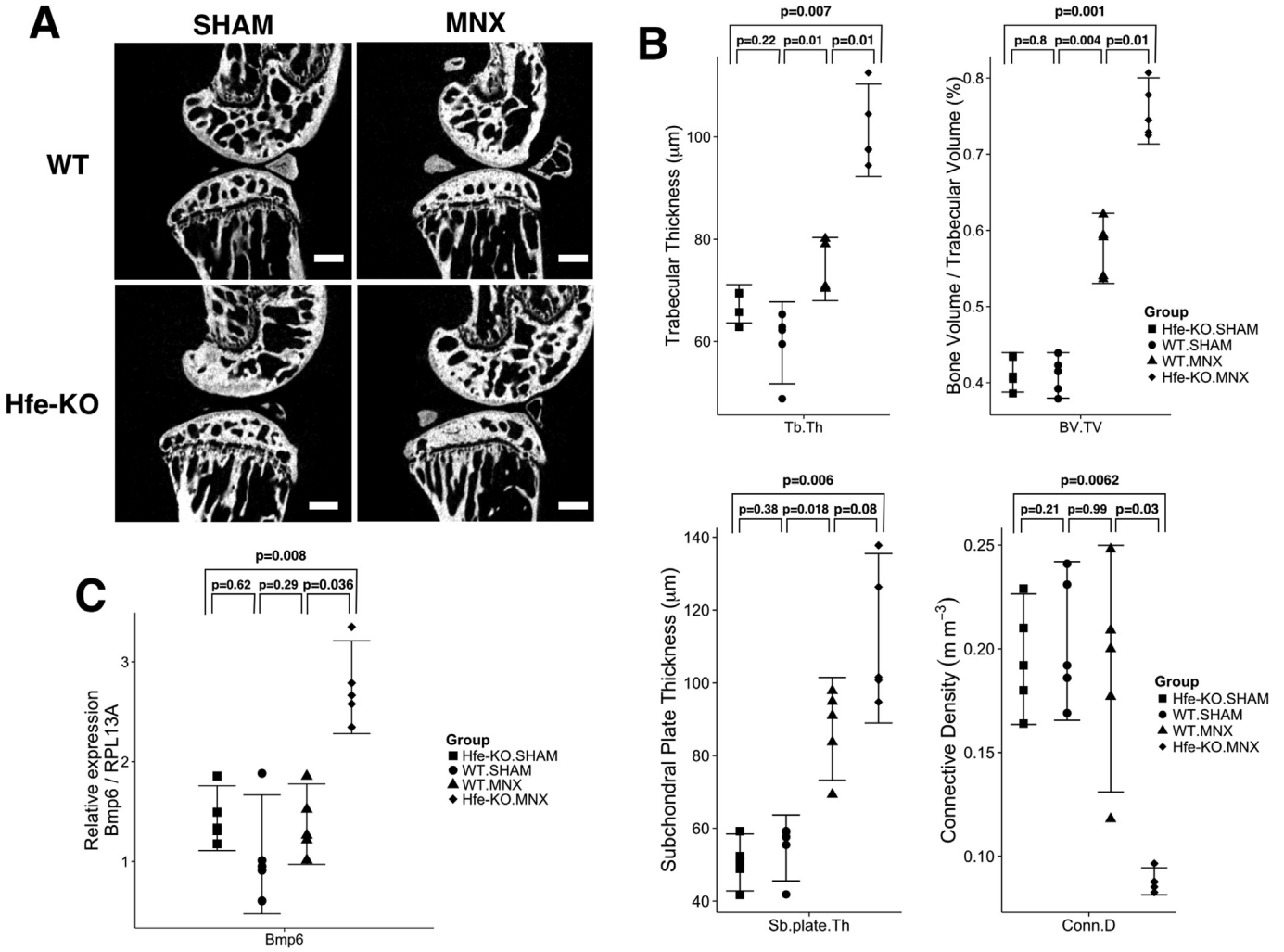


**Fig. 3.** Subchondral bone changes following meniscectomy in WT and Hfe-KO mice (A) Knee micro-CT sagittal reconstructions at the level of the middle one-third medial tibial plateau of control ($n = 5$ per group) and Hfe-KO mice ($n = 5$ per group) at 8 weeks after surgical induction of OA. Scale bar 500 µm (B) Quantification of microarchitecture parameters of the medial tibial plateau of mice knees ($n = 5$ per group). The results show that the MNX operated knees of the Hfe-KO animals have a greater degree of subchondral sclerosis when compared to their WT controls. Data are shown as the individual values (shapes) with the corresponding 95% CI (range) (C) Real time PCR, using mRNA isolated from the medial knee compartment of 18 weeks-old animals, to detect the expression of the *Bmp6* gene. The results show that MNX surgery leads to an increase in the expression of the gene but only in Hfe-KO mice is it significant. Data are the individual values (shapes) with the corresponding 95% CI (range).

operated knees had a similar percentage of articular chondrocytes positive for type X collagen, ADAMTS-5 and MMP-13, but the Hfe-KO, MNX operated knees displayed stronger staining and a greater percentage of MMP-3 positive cells when compared to their WT controls ($n = 3$ per group, Fig. 5).

## Discussion

This is the first study describing the effect of systemic iron overload in the development of OA *in vivo*, by analysing Hfe-KO mice. At eight weeks after surgical induction of OA, the Hfe-KO mice showed an accelerated OA progression associated to a greater cartilage destruction, greater subchondral bone volume and an increased expression of a gene related to cartilage degradation when compared to their wild-type controls.

As previously described[19], the mutation had no effect on the morphology of the mice but caused a significant systemic iron overload with increased iron content observed in the serum and liver of the Hfe-KO mice. Following arthrotomy the Hfe-KO mice showed an increased deposition of iron in the form of hemosiderin in the synovial membrane. Synovial iron accumulation can also be found in human HH patients and in patients with RA[11]. It is thought that the iron arises not from the exchange with the labile iron pool but from blood that enters the joint, either by trauma or by oozing from an inflamed synovial membrane[26]. Accordingly, we hypothesise that the iron seen in the knee synovial membrane would originate from blood entering the joint following the arthrotomy. The greater hemosiderin accumulation in the Hfe-KO mice joints could be therefore explained by the higher iron content of their blood.

By itself, iron accumulation in the synovial membrane does not appear to be enough to cause cartilage damage in this time period, as shown by the data from Hfe-KO mice SHAM-operated knees, since their histological, morphological and gene expression characteristics do not show any evidence of OA and are identical to their WT counterparts. Feeding the mice with an iron-enriched diet in order to obtain an even greater iron overload or having a longer follow-up period could yield different results.

Previous reports show that the levels of proinflammatory cytokines are elevated in the first days following injury[27,28] and then gradually decrease in the following weeks, eventually returning to normal levels[29,30]. This could explain the absence of significant differences in the expression of *Il1b* and *Il6* in this study since the

Please cite this article in press as: Camacho A, et al., Iron overload in a murine model of hereditary hemochromatosis is associated with accelerated progression of osteoarthritis under mechanical stress, Osteoarthritis and Cartilage (2015), http://dx.doi.org/10.1016/j.joca.2015.09.007

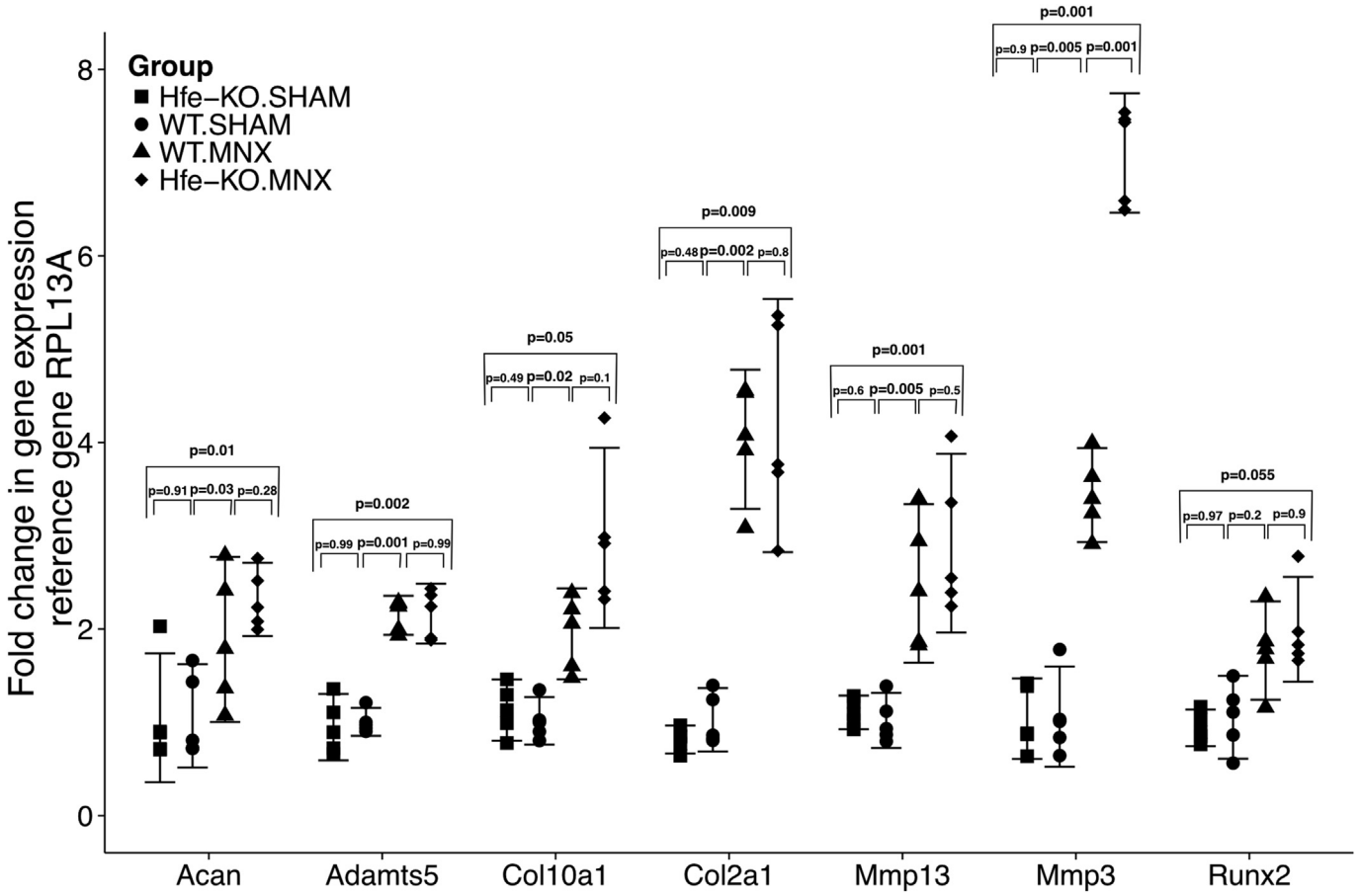


**Fig. 4.** Changes in gene expression following surgical induction of OA. Real time PCR, using mRNA isolated from the medial knee compartment of animals euthanized 8 weeks after surgery, to detect the expression of selected target genes ($n = 5$ per group). The results confirm that MNX surgery induces the expression of genes related with matrix degradation and chondrocyte hypertrophy and that this is more pronounced in the Hfe-KO mice. Data are shown as the individual values (shapes) with the corresponding 95% CI (range).

mice were evaluated at 8 weeks after the initial injury, when the disease process is already in a quiescent phase[31].

As previously reported in the literature, we found that surgically induced mechanical instability of the knee joint resulted in deregulation of genes related to extracellular matrix production, matrix degradation and chondrocyte hypertrophy[31–33], as well as cartilage degeneration[34,35] and subchondral bone sclerosis[36,37]. All of these were observable in both WT and Hfe-KO mice meniscectomized knees but differences were more evident in the latter (Figs. 1–4) providing further evidence for the increased susceptibility for OA in the Hfe-KO mice. On the other hand, the presence of excess iron in the synovial tissue could also account for the accelerated OA progression in the meniscectomized knees of the Hfe-KO mice since intra- and extra-cellular overload of iron in the tissue induces the generation of free radicals and reactive oxygen species (ROS)[38–40]. These can lead to hyper-activation of MMPs[41], a crucial step in many normal and pathological biological processes[42]. We observed that, following the surgical induction of OA, the Hfe-KO mice displayed an increased expression of MMP-3 when compared to their WT controls. MMP-3 is an enzyme capable of degrading several components of the extracellular matrix, making it less resilient to the mechanical stress and accelerating the progression of OA[33,43]. Therefore we hypothesise that the increased iron content in the synovial membrane contributes to an increased generation of ROS after an initial pro-inflammatory signal, such as joint trauma or surgical intervention, causing an up-regulation of MMP-3 expression, contributing to the greater cartilage damage observed in the Hfe-KO mice knees.

The precise role of subchondral bone in the initiation and progression of OA is still unclear[44,45]. A recent review[46] proposes that the non-physiologic strain on the joint causes micro damage to the subchondral bone leading to increased resorption and a decrease in thickness in the early-stages of OA, progressing to subchondral trabecular sclerosis and increased calcified cartilage thickness in the late-stage OA. These changes in subchondral bone architecture are likely to accompany cartilage damage that could, in turn, influence subchondral bone degradation, resulting in a vicious cycle. Accordingly, in our study we observed a greater increase in subchondral bone volume and calcified cartilage thickness in the joints with more pronounced cartilage damage, which was in agreement to data previously reported by Chappard *et al.*[47], Hayami *et al.*[48] and Botter *et al*[36].

The present study has some limitations. In humans, HH-related OA develops in the fourth and fifth decades of life whereas we used young mice (10-week-old) to study the development of OA therefore this model may not accurately represent the evolution of the human disease. The observed changes in cartilage and subchondral bone were restricted to a single time-point making it difficult to conclude about the entire sequence of changes leading to OA, but this could be addressed in future studies. The time point was chosen since the cartilage and subchondral bone changes are already well defined[18] and the disease process is in a quiescent phase[31]. Our selection of target genes was geared towards the main components of the extracellular matrix[49], the main proteolytic enzymes involved in matrix degradation[43,50] and the main molecules related with chondrocyte hypertrophy[51]. It is possible that

Please cite this article in press as: Camacho A, et al., Iron overload in a murine model of hereditary hemochromatosis is associated with accelerated progression of osteoarthritis under mechanical stress, Osteoarthritis and Cartilage (2015), http://dx.doi.org/10.1016/j.joca.2015.09.007

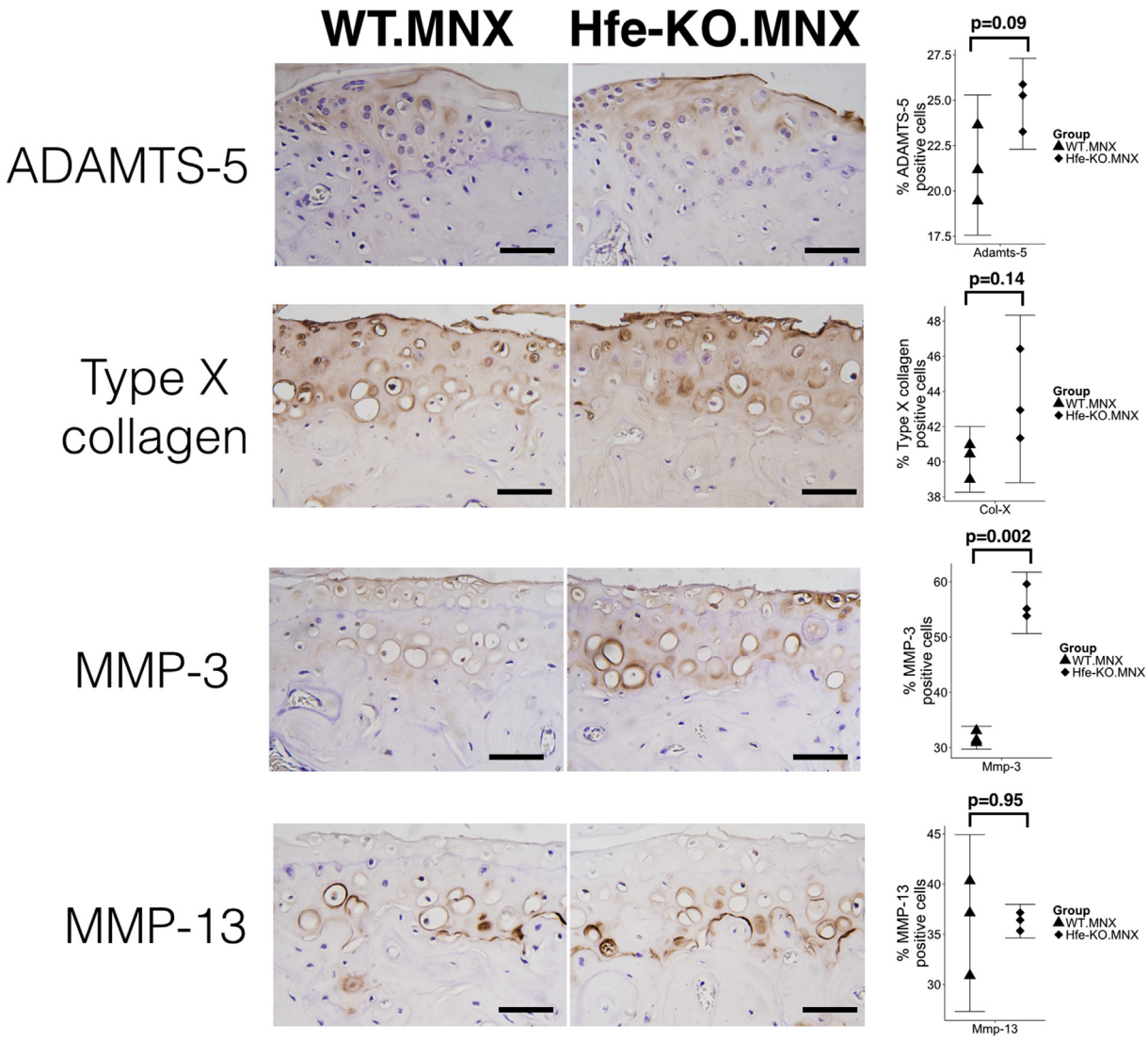


**Fig. 5.** Immunohistochemistry for, a disintegrin and metallopeptidase with thrombospondin motifs (ADAMTS-5), type X collagen, matrix metallopeptidase 3 (MMP-3) and matrix metallopeptidase 13 (MMP-13), in the medial tibial plateau at 8 weeks after MNX surgery in control (WT.MNX) and *Hfe*-KO (Hfe-KO.MNX) mice (3,3′-diaminobenzidine (DAB)) counterstained with Harris haematoxylin, scale bars = 50 μm). The ratio of positive cells per field was counted under a microscope at 40× magnification using three sections from three mice. The results show that MMP-3 is significantly more expressed in the Hfe-KO mice knees following MNX surgery. Data are the individual values (shapes) with the corresponding 95% CI (range).

other genes may also be relevant in the development of HH-related OA, this could also be addressed in future studies.

In conclusion, we found that HFE-KO mice are an interesting model for the study of HH-related OA since they developed accelerated knee OA progression after medial meniscectomy when compared to their WT controls, this could be secondary to the increased expression of MMP-3 observed in the iron-overloaded joints. Further studies regarding the pathway responsible for MMPs overexpression in iron-overloaded joints could provide a better insight into OA pathophysiology and lead to novel therapeutic targets.

## Contributors

The seven authors are justifiably credited with authorship, according to the authorship criteria. In detail: A. Camacho – conception, design, acquisition of data, analysis and interpretation of data, drafting of the manuscript, final approval given; M. Simão – acquisition of data, analysis and interpretation of data, final approval given. H.K. Ea – acquisition of data, critical revision of manuscript, final approval given; M. Cohen-Solal – design, critical revision of manuscript, final approval given; P. Richette – critical revision of manuscript, final approval given; J. Branco – critical revision of manuscript, final approval given; M.L. Cancela – conception, design, critical revision of manuscript, final approval given. A Camacho takes responsibility for the integrity of the work as a whole.

## Competing interests

None of the authors have financial or personal relationships with other people or organizations that could bias the work and conclusions stated in this manuscript.

## Funding

This research was partially supported by National Funds through FCT – Foundation for Science and Technology, under the project "CCMAR/Multi/04326/2013". M. Simão was supported by a doctoral grant from FCT (SFRH/BD/77056/2011).

Please cite this article in press as: Camacho A, et al., Iron overload in a murine model of hereditary hemochromatosis is associated with accelerated progression of osteoarthritis under mechanical stress, Osteoarthritis and Cartilage (2015), http://dx.doi.org/10.1016/j.joca.2015.09.007

The funding source had no influence on the study design, data collection, analysis and interpretation, nor in the writing of the manuscript or the decision to submit it.

## Acknowledgments

We thank Caroline Marty at INSERM 1132 and Paulo Gavaia at CCMAR for their technical expertise with histochemical techniques and Agnès Ostertag at INSERM 1132 for assistance with the micro-CT scanner and software. Also the authors thank the late Jorge Pinto at Instituto de Biologia Molecular e Celular (IBMC) in Porto for providing the initial colony of Hfe-KO mice.

## Supplementary data

Supplementary data related to this article can be found at http://dx.doi.org/10.1016/j.joca.2015.09.007.

## References

1. Johnson VL, Hunter DJ. The epidemiology of osteoarthritis. Best Pract Res Clin Rheumatol 2014;28:5–15.
2. Neogi T, Zhang Y. Epidemiology of osteoarthritis. Rheum Dis Clin North Am 2013;39:1–19.
3. Loeser RF, Goldring SR, Scanzello CR, Goldring MB. Osteoarthritis: a disease of the joint as an organ. Arthritis Rheum 2012;64:1697–707.
4. Zhou XY, Tomatsu S, Fleming RE, Parkkila S, Waheed A, Jiang J, *et al*. HFE gene knockout produces mouse model of hereditary hemochromatosis. Proc Natl Acad Sci 1998;95:2492–7.
5. Pietrangelo A. Hereditary hemochromatosis: pathogenesis, diagnosis, and treatment. Gastroenterology 2010;139:393–408. 408.e391-392.
6. Richette P, Ottaviani S, Vicaut E, Bardin T. Musculoskeletal complications of hereditary hemochromatosis: a case-control study. J Rheumatol 2010;37:2145–50.
7. Elmberg M, Hultcrantz R, Simard JF, Carlsson Å, Askling J. Increased risk of arthropathies and joint replacement surgery in patients with genetic hemochromatosis: a study of 3,531 patients and their 11,794 first-degree relatives. Arthritis Care Res (Hoboken) 2013;65:678–85.
8. Sahinbegovic E, Dallos T, Aigner E, Axmann R, Engelbrecht M, Schöniger-Hekele M, *et al*. Hereditary hemochromatosis as a risk factor for joint replacement surgery. Am J Med 2010;123:659–62.
9. Wang Y, Gurrin LC, Wluka AE, Bertalli NA, Osborne NJ, Delatycki MB, *et al*. HFE C282Y homozygosity is associated with an increased risk of total hip replacement for osteoarthritis. Semin Arthritis Rheum 2012;41:872–8.
10. von Kempis J. Arthropathy in hereditary hemochromatosis. Curr Opin Rheumatol 2001;13:80–3.
11. Heiland GR, Aigner E, Dallos T, Sahinbegovic E, Krenn V, Thaler C, *et al*. Synovial immunopathology in haemochromatosis arthropathy. Ann Rheum Dis 2010;69:1214–9.
12. Schumacher HR. Articular cartilage in the degenerative arthropathy of hemochromatosis. Arthritis Rheum 1982;25:1460–8.
13. Carroll GJ, Sharma G, Upadhyay A, Jazayeri JA. Ferritin concentrations in synovial fluid are higher in osteoarthritis patients with HFE gene mutations (C282Y or H63D). Scand J Rheumatol 2010;39:413–20.
14. Husar-Memmer E, Stadlmayr A, Datz C, Zwerina J. HFE-related hemochromatosis: an update for the rheumatologist. Curr Rheumatol Rep 2014;16:393.
15. Nicolas G, Viatte L, Lou D-Q, Bennoun M, Beaumont C, Kahn A, *et al*. Constitutive hepcidin expression prevents iron overload in a mouse model of hemochromatosis. Nat Genet 2003;34:97–101.
16. Cooksey RC, Jouihan HA, Ajioka RS, Hazel MW, Jones DL, Kushner JP, *et al*. Oxidative stress, beta-cell apoptosis, and decreased insulin secretory capacity in mouse models of hemochromatosis. Endocrinology 2004;145:5305–12.
17. Guggenbuhl P, Fergelot P, Doyard M, Libouban H, Roth M-P, Gallois Y, *et al*. Bone status in a mouse model of genetic hemochromatosis. Osteoporos Int 2011;22:2313–9.
18. Kamekura S, Hoshi K, Shimoaka T, Chung U, Chikuda H, Yamada T, *et al*. Osteoarthritis development in novel experimental mouse models induced by knee joint instability. Osteoarthritis Cartilage 2005;13:632–41.
19. Levy JE, Montross LK, Cohen DE, Fleming MD, Andrews NC. The C282Y mutation causing hereditary hemochromatosis does not produce a null allele. Blood 1999;94:9–11.
20. Rebouche CJ, Wilcox CL, Widness JA. Microanalysis of non-heme iron in animal tissues. J Biochem Biophys Methods 2004;58:239–51.
21. Glasson SS, Chambers MG, Van Den Berg WB, Little CB. The OARSI histopathology initiative – recommendations for histological assessments of osteoarthritis in the mouse. Osteoarthritis Cartilage 2010;18(Suppl 3):S17–23.
22. Botter SM, van Osch GJVM, Waarsing JH, Day JS, Verhaar JAN, Pols HAP, *et al*. Quantification of subchondral bone changes in a murine osteoarthritis model using micro-CT. Biorheology 2006;43:379–88.
23. Curtis KM, Gomez LA, Rios C, Garbayo E, Raval AP, Perez-Pinzon MA, *et al*. EF1alpha and RPL13a represent normalization genes suitable for RT-qPCR analysis of bone marrow derived mesenchymal stem cells. BMC Mol Biol 2010;11:61.
24. Andriopoulos Jr Billy, Corradini E, Xia Y, Faasse SA, Chen S, Grgurevic L, *et al*. BMP6 is a key endogenous regulator of hepcidin expression and iron metabolism. Nat Genet 2009;41:482–7.
25. Kugimiya F, Kawaguchi H, Kamekura S, Chikuda H, Ohba S, Yano F, *et al*. Involvement of endogenous bone morphogenetic protein (BMP) 2 and BMP6 in bone formation. J Biol Chem 2005;280:35704–12.
26. Muirden KD, Senator GB. Iron in the synovial membrane in rheumatoid arthritis and other joint diseases. Ann Rheum Dis 1968;27:38–48.
27. Haslauer CM, Proffen BL, Johnson VM, Hill A, Murray MM. Gene expression of catabolic inflammatory cytokines peak before anabolic inflammatory cytokines after ACL injury in a preclinical model. J Inflamm (Lond) 2014;11:34.
28. Irie K, Uchiyama E, Iwaso H. Intraarticular inflammatory cytokines in acute anterior cruciate ligament injured knee. Knee 2003;10:93–6.
29. Bigoni M, Sacerdote P, Turati M, Franchi S, Gandolla M, Gaddi D, *et al*. Acute and late changes in intraarticular cytokine levels following anterior cruciate ligament injury. J Orthop Res 2013;31:315–21.
30. Ward BD, Furman BD, Huebner JL, Kraus VB, Guilak F, Olson SA. Absence of posttraumatic arthritis following intraarticular fracture in the MRL/MpJ mouse. Arthritis Rheum 2008;58:744–53.
31. Loeser RF, Olex AL, McNulty MA, Carlson CS, Callahan M, Ferguson C, *et al*. Disease progression and phasic changes in gene expression in a mouse model of osteoarthritis. PLoS One 2013;8:e54633.
32. Appleton CTG, Pitelka V, Henry J, Beier F. Global analyses of gene expression in early experimental osteoarthritis. Arthritis Rheum 2007;56:1854–68.

Please cite this article in press as: Camacho A, et al., Iron overload in a murine model of hereditary hemochromatosis is associated with accelerated progression of osteoarthritis under mechanical stress, Osteoarthritis and Cartilage (2015), http://dx.doi.org/10.1016/j.joca.2015.09.007

33. Bateman JF, Rowley L, Belluoccio D, Chan B, Bell K, Fosang AJ, *et al*. Transcriptomics of wild-type mice and mice lacking ADAMTS-5 activity identifies genes involved in osteoarthritis initiation and cartilage destruction. Arthritis Rheum 2013;65:1547–60.
34. Burleigh A, Chanalaris A, Gardiner MD, Driscoll C, Boruc O, Saklatvala J, *et al*. Joint immobilization prevents murine osteoarthritis and reveals the highly mechanosensitive nature of protease expression in vivo. Arthritis Rheum 2012;64:2278–88.
35. Glasson SS, Blanchet TJ, Morris EA. The surgical destabilization of the medial meniscus (DMM) model of osteoarthritis in the 129/SvEv mouse. Osteoarthritis Cartilage 2007;15:1061–9.
36. Botter SM, Glasson SS, Hopkins B, Clockaerts S, Weinans H, van Leeuwen JPTM, *et al*. ADAMTS5-/- mice have less subchondral bone changes after induction of osteoarthritis through surgical instability: implications for a link between cartilage and subchondral bone changes. Osteoarthritis Cartilage 2009;17:636–45.
37. Hayami T, Pickarski M, Wesolowski GA, McLane J, Bone A, Destefano J, *et al*. The role of subchondral bone remodeling in osteoarthritis: reduction of cartilage degeneration and prevention of osteophyte formation by alendronate in the rat anterior cruciate ligament transection model. Arthritis Rheum 2004;50:1193–206.
38. Brissot P, Ropert M, Le Lan C, Loréal O. Non-transferrin bound iron: a key role in iron overload and iron toxicity. Biochim Biophys Acta 2012;1820:403–10.
39. Morris CJ, Blake DR, Wainwright AC, Steven MM. Relationship between iron deposits and tissue damage in the synovium: an ultrastructural study. Ann Rheum Dis 1986;45:21–6.
40. Sullivan JL. Is stored iron safe? J Lab Clin Med 2004;144:280–4.
41. Mairuae N, Connor JR, Cheepsunthorn P. Increased cellular iron levels affect matrix metalloproteinase expression and phagocytosis in activated microglia. Neurosci Lett 2011;500:36–40.
42. Nagase H, Woessner JF. Matrix metalloproteinases. J Biol Chem 1999;274:21491–4.
43. Blom AB, van Lent PL, Libregts S, Holthuysen AE, van der Kraan PM, van Rooijen N, *et al*. Crucial role of macrophages in matrix metalloproteinase-mediated cartilage destruction during experimental osteoarthritis: involvement of matrix metalloproteinase 3. Arthritis Rheum 2007;56:147–57.
44. Burr DB. The importance of subchondral bone in the progression of osteoarthritis. J Rheumatol Suppl 2004;70:77–80.
45. Oegema Jr TR, Carpenter RJ, Hofmeister F, Thompson Jr RC. The interaction of the zone of calcified cartilage and subchondral bone in osteoarthritis. Microsc Res Tech 1997;37:324–32.
46. Li G, Yin J, Gao J, Cheng TS, Pavlos NJ, Zhang C, *et al*. Subchondral bone in osteoarthritis: insight into risk factors and microstructural changes. Arthritis Res Ther 2013;15:223.
47. Chappard C, Peyrin F, Bonnassie A, Lemineur G, Brunet-Imbault B, Lespessailles E, *et al*. Subchondral bone micro-architectural alterations in osteoarthritis: a synchrotron micro-computed tomography study. Osteoarthritis Cartilage 2006;14:215–23.
48. Hayami T, Pickarski M, Zhuo Y, Wesolowski GA, Rodan GA, Duong LT. Characterization of articular cartilage and subchondral bone changes in the rat anterior cruciate ligament transection and meniscectomized models of osteoarthritis. Bone 2006;38:234–43.
49. Martin I, Jakob M, Schäfer D, Dick W, Spagnoli G, Heberer M. Quantitative analysis of gene expression in human articular cartilage from normal and osteoarthritic joints. Osteoarthritis Cartilage 2001;9:112–8.
50. Verma P, Dalal K. ADAMTS-4 and ADAMTS-5: key enzymes in osteoarthritis. J Cell Biochem 2011;112:3507–14.
51. Zheng Q, Zhou G, Morello R, Chen Y, Garcia-Rojas X, Lee B. Type X collagen gene regulation by Runx2 contributes directly to its hypertrophic chondrocyte-specific expression in vivo. J Cell Biol 2003;162:833–42.


Please cite this article in press as: Camacho A, et al., Iron overload in a murine model of hereditary hemochromatosis is associated with accelerated progression of osteoarthritis under mechanical stress, Osteoarthritis and Cartilage (2015), http://dx.doi.org/10.1016/j.joca.2015.09.007